# Tension-Saturated and Unsaturated Flows from Line Sources in Subsurface Irrigation: Riesenkampf's and Philip's Solutions Revisited

*A.R.Kacimov*[1], *Yu.V.Obnosov*[2],

[1]Department of Soils, Water and Agricultural Engineering, Sultan Qaboos University, Oman

anvar@squ.edu.om, akacimov@gmail.com

[2]Institute of Mathematics and Mechanics, Kazan Federal University, Kazan, Russia

yobnosov@kpfu.ru

**Key points:**

Steady 2D flow from buried line sources is analytically studied

Green-Ampt and quasilinear model are compared.

**Abstract**. Riesenkampf's (1938), R-38 (referred to here as R-38), analytical solution for steady 2-D flow from a buried line source in a homogeneous Green-Ampt soil, with a wetting plume bounded by a free surface (capillary fringe), is compared with Philip's (1969), (P-69), one for genuinely-unsaturated wetting of Gardner's infinite-extension soil. Conformal mappings are used in R-38, from which we derived the flow net, pore-water isobars, isochrones, fields of Darcian velocity and resultant force acting on saturated porous skeleton, fine geometry (shape and size) of the constant-head contour encompassing a mole-emitter or leaky-pipe, as well as the dependence of the total discharge per unit pipe length on uniform pressure in the pipe, capillarity of the soil, radius of the pipe and saturated hydraulic conductivity. An ovalic "water table" isobar, encompassing P-69 source, is compared with one of R-38 for a fixed discharge and saturated conductivity but adjusted sorptive numbers. The Whisler-Bouwer (1970) relation between the static height of capillary rise and sorptive number is shown to give a good match between R-38 and P-69 isobars. This allows to use R-38 in the source vicinity and P-69 in the far-field zone. Computer algebra (*Mathematica*) routines are used for visualization of the known and extended R-38 and P-69 solutions.

**Key words: complex potential, Zhukovsky function, flow net – isobars - isotachs - isochrones, pipe discharge, sorptive number versus air-entrance pressure, ADE for Kirchhoff's potential.**

## 1. Introduction

Subsurface irrigation (SI) supplies water to the plant roots from emitters placed along a pipe (tube) buried at a certain depth (normally 5-100 cm) under the soil surface. Porous pipes made of clay or re-processed waste materials are also called "leaky pipes" or "*Aquapores*" (see e.g. Teeluck and Sutton, 1998) and they uniformly emit through pipe walls. In cohesive clayey soils just mole-type holes are also ploughed by torpedo-shaped foot with a cylindrical expander, without any pipe (casing). Water is injected into these holes and seeps directly into the adjacent soil without a skin-effect (extra wall-resistance). A typical discharge of SI pipes is seldom more than few hundred liters per day per meter and the pressure in the pipe seldom exceeds several tens of thousands of kPa. Seepage from the pipe, with or without skin-effect, generates a positive pressure, a full saturation zone around the pipe and an unsaturated zone far from the source such that crops' roots thrive (Fig.1a represents a vertical cross section of a seepage flow domain).

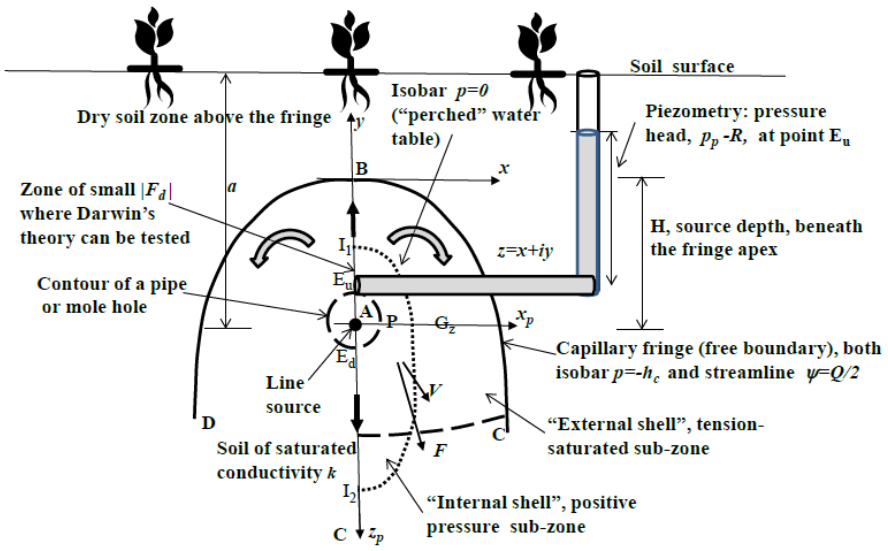


Fig.1a. Vertical cross section of a seepage flow domain.

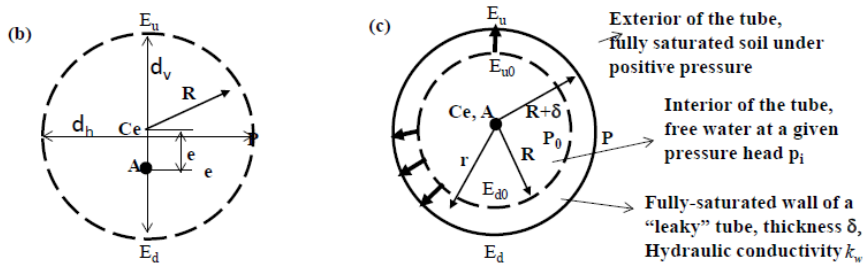


Fig.1b,c Zoomed near-source zone (b). Leaky pipe with permeable wall (c).

Agroengineering advantages of SI, as compared with surface drippers, furrows, sprinklers and border irrigation are: reduced irrigation norms and water saving, trimmed evaporation, excluded runoff and ensued topsoil erosion, no direct contact of irrigation water of marginal quality with the foliage, minimized mosquito breeding, more efficient fertigation and application of pesticides, better weed control, improved plant health due to lower air humidity of the canopy zone, no top soil crust formation due to impact of water droplets, no petit larceny of irrigation gadgets, reduced pest damage, among others (see e.g. Ayars, et al., 2015, Camp, 1998, Lamm and Camp, 2007, Lamm et al., 2012). Two brothers, Prof. Bruno Riesenkampf (http://math.sgu.ru/historychair.php?id=3&lang=ru) and Prof. George Riesenkampf

(http://www.vniig.rushydro.ru/company/history/istoriya-vniig-v-litsakh/94710.html), contributed to SI projects in the 1920-1930–th by developing mathematical models of seepage and implementation of these models into agricultural engineering design in Russia.

Porous SI leaky pipes showed high efficiency, as compared with more common surface emitters, in many arid regions, e.g. in Oman and Saudi Arabia (Al-Rawahy et al., 2004, El-Nesr et al., 2014). A recent boost to SI has come from the last California drought, after which the interest skyrocketed in smart root-zone wetting and thrifty usage of dwindling water resources in the vadose zone and aquifers.

Among disadvantages of SI, the most important ones are relevant to dynamics of water in the subsurface:

- topology of seepage flow from a buried source can be hydroecologically unfavourable, e.g. the wetted zone may be too small and/or below the root zone, especially in coarse-textured soils; the upward motion of water from the source may be too weak so that most water is lost to deep percolation downwards with no benefit to the plants that is critical at the stage of germination
- the hydraulic gradients (Darcian velocities) near the source (A in Fig.1a) can be so high that the fine fractions of the soil are entrained by seepage and drift down with pernicious consequences for the soil texture
- the water emitted from the source can cause excessive upward water motion and - in arid climates - the associated transport of dissolved salts causing secondary salinization of the topsoil and root zone

Mathematical modeling and experiments with SI from leaky pipes and other emitters have been done for cascades and arrays of sources, transient flow conditions (irrigation pulses) and solute dynamics near emitters (see, e.g. Ashrafi et al., 2002, Cook et al., 2003, Diamantopoulos and Elmaloglou, 2012, El-Nesr et al., 2014, Emikh, 1999a,b, Gupta et al., 2009, Kasimov, 1992, Lubana and Narda, 2001, Martínez and Reca, 2014, Mmowala and Or, 2000, Naglič et

al., 2014, Siyal and Skaggs, 2009, Siyal et al., 2013, Strack, 1989, Subbaiah, 2013) for soils of different hydraulic and capillary properties, radii of pipes, emitting rates, flow domains and heterogeneities of the soil. In numerical modeling the HYDRUS-2,3D package has been often used, i.e. the governing Richards equation was solved by FEM, involving the famous triad of VG capillary parameters. The analytical solutions were not fully utilized by the masters of HYDRUS. Therefore, in this paper we try to fill in this lacuna between the modern numerical-experimental modeling and analytical solutions. Namely, we utilize two analytical models for seepage from line sources under steady-state regimes in unbounded soils: the Riesenkampf (1938) (hereafter abbreviated as R-38) and Philip (1969) (hereafter abbreviated as P-69) solutions, with a plume of later papers referenced below.

The Laplace and steady advective dispersion equations (ADE) for the hydraulic head and Kirchhoff potential, govern the flow in R-38 and P-69, respectively. The emitting pipe is modeled as a mathematical source, which has infinitely high pressure at the locus of the placed singularity. The pressure decreases

rapidly away from the center. Practically the pipe (lateral) is of a finite size (diameter) and under a finite pressure. In both analytical solutions using the Green and Ampt and Gardner's soil models and boundary-value problems for two different PDEs, the analysis of the near-pipe flow zone and comparisons of the two models has not been done. This is the first objective of our paper: to find out for which pipe sizes, pipe pressures, discharges and soil characteristics the R-38 and P-69 models are applicable and where the two sets of analytical formulae converge.

Another objective of this work is to present a detailed analysis of the following flow characteristics of the R-38 solution: the flow net, velocity, pressure and seepage force fields, and travel time of marked particles moving along streamlines, comparing them with P-69.

In R-38 and P-69 the source discharge was given that allowed to solve the Laplace equation and ADE. The relationship between the discharge and pipe pressure was not, however, established by R-38 and P-69. This is the third objective of our paper.

In numerical models and experiments (see e.g. Gupta et al., 2008, Siyal and Skaggs, 2009, Teeluck and Sutton, 1998) real "leaky" pipes, whose walls have a finite permeability, were investigated. Analytical solutions of R-38 and P-69 ignore wall's hydraulic resistance to seepage. The fourth objective is to amend R-38 with a "skin effect" of the buried pipe.

## 2. Computation of Flow Characteristics in Tension-Saturated Flow Bounded by Capillary Fringe

A mole drain or porous tube of a small radius $R$ is laid at a depth $a$ beneath the ground surface (Fig.1a shows a vertical cross-section of one lateral of the whole irrigated field); there is no interference of flow from neighbouring laterals. Soil's saturated hydraulic conductivity is $k$ and static capillary height is $h_c$ (both are constants for a given soil and are tabulated in Polubarinova-Kochina, 1962, 1977, hereafter abbreviated as PK-62,77). Positive pressure head, $p_p$, in the pipe centre is maintained from a main. Ideally, along the tube $p_p$ should be uniform despite losses to seepage into the soil; discharge, $Q$, becomes steady after a short period of "infiltration-type" adjustment when the pipe is filled with water and is also constant along the pipe axis.

Seepage is modeled by a line source (mathematical singularity) of a constant strength $Q$ (see R-38, PK-62,77) which generates a flow zone consisting of a fully saturated (positive pressure head) "internal shell" adjacent to the leaky tube and an "external shell" of tension-saturated zone adjacent to the "internal shell" (see our Fig.1a and Figures 1-3, 5-7 from Warrick and Zhang, 1987 in a similar furrow irrigation problem).

In this section we utilize the Green-Ampt model developed by Vedernikov (1939) for steady-state 2-D tension-saturated flows. R-38 applied this model to subsurface line emitters. Flow is bounded by a capillary fringe *DBC* (Fig.1a). Along this *apriori* unknown curve (free boundary) pressure head attains its minimum value within the flow domain, $p=-h_c$. Nikolskii (1961) and Emikh (1999 a,b) extended R-38 analysis to cases of a constant head horizon under (substratum)

or above (exfiltration strip) the source. Transient solutions were obtained by Chu (1994), and Sepaskhah and Chitsaz (2004). Strack (1989) obtained steady solutions for an arbitrary number of sources (emitting pipes) and sinks (drains). These arrays of SI-drainage can be utilized if the wetted area for crop roots is insufficient. In this paper we focus on a single emitting line to carry out a fine-tuned analysis of the near-emitter and far-field zones.

In Appendix, we repeat the derivations of R-38 (see also PK-62,77) with minor amendments, *viz.* we map conformally the strip of the complex potential domain (Fig.2a) onto the half-strip of the Zhukovsky domain (Fig.2b) via an auxiliary plane Fig.(2c).

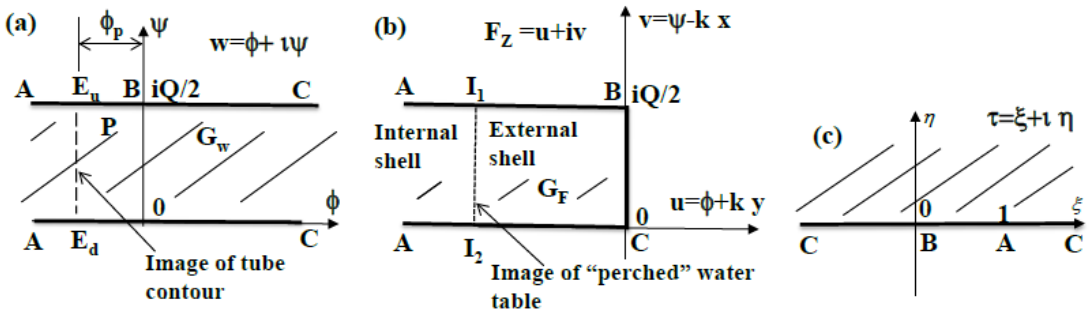


Fig.2 Complex potential domain (a); Zhukovsky function domain (b); auxiliary half-plane (c).

Below we use computer algebra - Wolfram's (1991) *Mathematica* - and do what R-38 and PK-62,77 could not in the epoch when such powerful packages were not available.

## *2.1 Flow net*

Similarly to Philip (1989) and R-38, we introduce the dimensionless quantities: $Z=X+iY=k\,z/Q$, $p_d=k\,p/Q$, $h_d=k\,h/Q$, $h_{cd}=k\,h_c/Q$, $V_d=V/k$ and $W=\Phi+i\,\Psi=w/Q$.

We put eqn.(A8) into eqn.(A5), with the help of **Re** and **Im** routines of *Mathematica* separate there the real and imaginary parts, and use the **ParametricPlot** routine to plot the flow net as Fig.3.

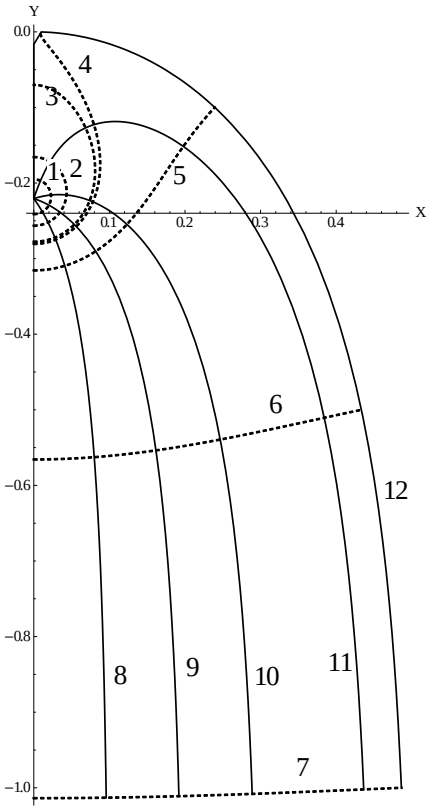


Fig.3. Flow net of R-38 point source solution (seven streamlines and five equipotential lines).

Here the constant total head contours $h_d$ = 0.2, 0.1, 0.01, 0, -0.1, - 0.5, -1 are shown by dashed lines, labeled 1-7, correspondingly. Solid lines in Fig.3 are Ψ=0.1, 0.2, 0.3, 0.45 and 0.5 (curves 8-12, correspondingly). It is noteworthy that at the stagnation point *B*, the stream line 12 swerves at an angle of $90^o$, the constant head line 4 is not orthogonal to the streamline 12 but rather makes an angle of $45^o$ at point *B*. This is caused by the loss of conformality of the mappings at this particular point. Positive *h* lines (within the contour 4) do not intersect the free surface (curve 12); close to the source at $Y_A$=-0.22 these curves are almost circular that actually allows to use the source solution for modeling leaky pipes. At very negative *Y* and total heads the corresponding contours are almost horizontal, streamlines are vertical and flow is unidirectionally descending, with pressure head close to $-h_c$.

Strack (1989, p.575) computed the streamlines for a more general case of two emitters and two interceptor drains. He used the Newton-Raphson procedure to solve a system of nonlinear equations by tracing streamlines in an auxiliary plane.

## *2.2. Velocity Field and Resultant Force*

Determination of the field of Darcian velocity, hydraulic gradient, forces acting on soil particles and massifs are vitally important for analysis of stability and sustainability of soils, as emphasized throughout PK-62,77. While seepage analysis in geotechnical engineering is a precursor to any design of hydraulic structures, in SI the potential impact on the soil matrix (postulated to be rigid) is usually ignored.

From eqns.(A5), (A7) and (A8) with the help of the **ParametricPlot** routine we plot the distribution of the velocity magnitude $|V_d|(\Phi)$ along streamlines selected in the range $0 < \psi_c < 1/2.$ The results are shown in Fig.4a for $\psi_c = 0,\ 0.2,\ 0.4,\ 0.45,\ 0.5$ (curves 1-5 correspondingly). The arc length (counted from the source) is:

$$s(\phi) = \int_0^{\Phi} \sqrt{[x'(\mu,\psi_c)]^2 + [y'(\mu,\psi_c)]^2}\, d\mu \qquad (1)$$

and Fig.4a can be easily replotted as $|V_d|(s)$.

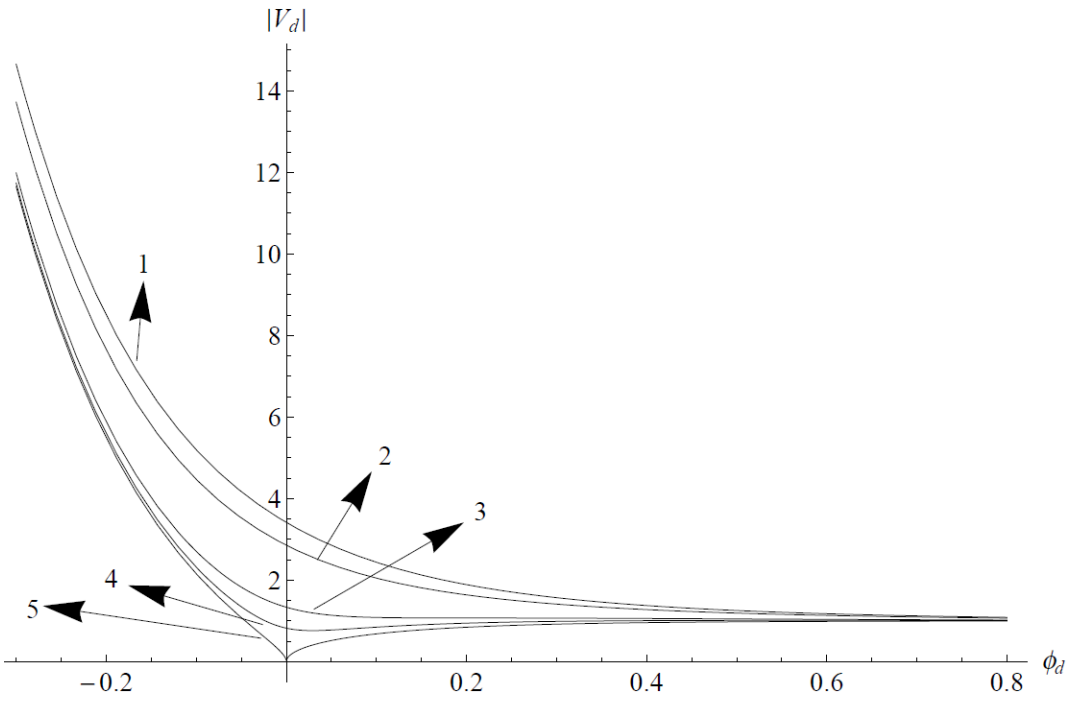

Fig.4a. Magnitude of dimensionless velocity (hydraulic gradient) along streamlines.

As we can see from Fig.4a, at $\psi < \psi_c = 0.39$ the magnitude of velocity decreases monotonically from infinity (source) to 1 (geometrical infinity). At $\psi > \psi_c$ there is a minimum of velocity at a certain point on the streamline although the asymptotic value at infinity is the same, i.e. 1. Close to the source, the hydraulic gradients are extremely high but the orientation of the velocity is from the pipe towards the soil, i.e. unlike mole drains, where the gradients are oriented towards the pipe, seepage does not cause collapse of the hole. However, as is well-known from the theory of suffusion (see e.g. PK-62, 77), at hydraulic gradients higher than about 1 the fine particulates of the soil are entrained by seepage, i.e. migrate along the streamlines. In cased groundwater and oil abstraction wells this results in formation damage (i.e. fine rock particles accumulate near perforations in casing or screen slots, see Obnosov et al., 2010). In emitting irrigation sources the fine particles are pushed away from point *A* in Fig.1a that increases the near tube permeability of the soil and "effective radius" of the irrigating tube. However, the change of texture and seepage-induced spatial heterogeneity of *k* near the pipe may have several deleterious consequences. Another threat of high gradients is "boiling" or heaving of the top soil above the emitter. If the depth *a* is too small and water extravasates (as e.g. in flow regimes of Emikh, 1999a), then the seepage-triggered uplift of soil becomes evident even for an unarmed eye. R-38 put forward a theory of forces-stresses in saturated porous media (see a summary in PK-62,77 and extension in Raats, 1968) . In particular, the resultant vector of force $\vec{F}$ [(see Fig.1a) exerted within a REV on solid particles in saturated porous medium is:

$$\vec{F} = \gamma \frac{\vec{V}}{k} - (1-m)(\gamma_s - \gamma)\,\vec{j}$$

where $\vec{V}$ is the vector of Darcian velocity $\gamma_s, \gamma$ are specific weights of solid particles and water respectively, *m* is porosity and $\vec{j}$ is the unit vector in the vertical direction. The last equation

for common water and sand particles density (most topsoils in Oman are sandy) and $m$=0.4 is reduced to a dimensionless form

$$\vec{F}_d \cong \vec{V}_d - \vec{j} \qquad (2)$$

where $\vec{F}_d = \vec{F}/\gamma$. With the help of eqn.(A7), from eqn.(2) we introduce a complex function $F_d(z) = V_d(z) - i$ .

Therefore, using this function, from the velocity field we immediately get the field of resultant force. Fig.4b shows the magnitude of $F_d$ as a function of the velocity potential along the same streamlines as in Fig.4a. From Fig.4b we see that far from the source $|F_d| \to 2$ along all streamlines i.e. where flow becomes vertical. For streamlines close to AC in Fig.1a, this asymptotic limit is monotonically attained. Along streamlines close to AB there is a single minimum of $|F_d|$. The minimum is zero along AB. Therefore, in the vicinity of this minimum-force point the skeleton is in "suspended" ("perfect quicksand"), weightless conditions. This zone could be a good candidate to test Darwin's-1880 paradigm of geotropism (see e.g. Hawes et al., 2002). Indeed, the hairs of plant roots reaching the zone of small $|F_d|$ above the source in Fig.1a will be a "solid" (but "adjustable") component of a "suspended" skeleton (alas, the soil skeleton with hairs is then not perfectly homogeneous with respect to $k$ as R-38 requires). Darwin's gravity factor is here eliminated by the upward hydraulic gradient. If the tips of the root hairs do not show preferential orientation downward, then Darwin was right. In other words, crop roots topology, formed under the R-38 seepage topology, in Oman (arid climate and no intervention of uncontrolled descending infiltration events after rainfalls) can confirm (or falsify) fundamentals of plant physiology.

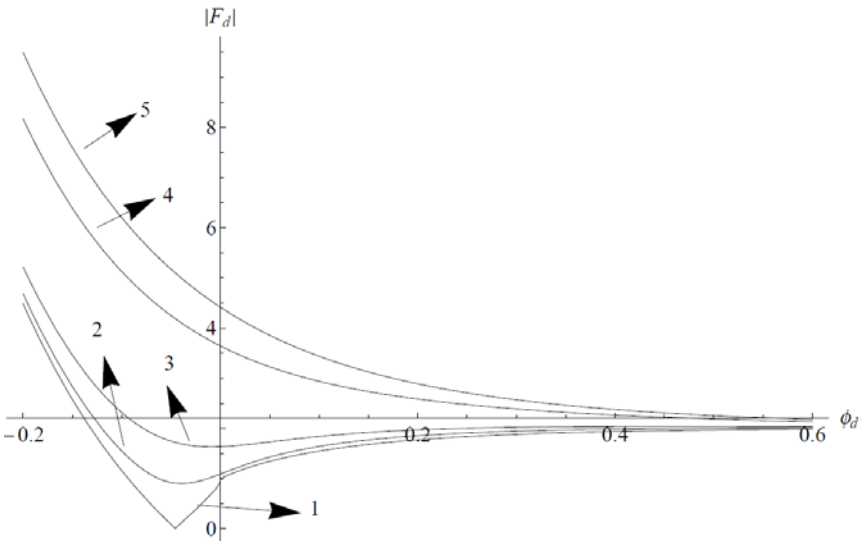


Fig.4b. Magnitude of dimensionless resultant force acting on a skeleton particle within a REV.

## *2.3 Determination of Discharge*

Now we rescale the R-38 solution in another manner. In real irrigation practice, the value of $p_p$ is known and $Q$, as well as $H$ according to eqn.(A6), is not (see e.g. Teeluck and Sutton, 1998). So, below we express $Q$ through $p_p$ in the following manner. We apply eqn.(A3) at point $E_u$ (the apex of the equipotential contour modeling the leaky pipe contour) where $\phi=-kh_p$ , $\psi=Q/2$, $\tau=1-\exp[-2\pi kh_p/Q]$, $z=-i(H-R)$. We put these values into eqn.(3) and take into account eqns.(A2) and (A6) to get the following nonlinear equation:

$$\frac{Q}{\pi k}\log 2 - R = \frac{Q}{\pi k}\log\left[1+\sqrt{1-\exp\left(\frac{-2\pi k\left(p_p + h_c - \frac{Q}{\pi k}\log 2\right)}{Q}\right)}\right] \qquad (3)$$

with respect to $Q$. Unlike R-38 and P-69 (they assumed $Q$ to be given), we introduce here new dimensionless variables: $Q^*=Q/(k\,h_c)$, $R^*=R/h_c$, $p_p{}^*=p_p/h_c$, $H^*=H_p/h_c$. $h^*=h/h_c$. Next, we use the **FindRoot** routine of *Mathematica* to solve eqn.(3). Fig.5 shows $Q^*(p_p{}^*)$ for $R^*$=0.01, 0.3, 0.7 (curves 1-3).

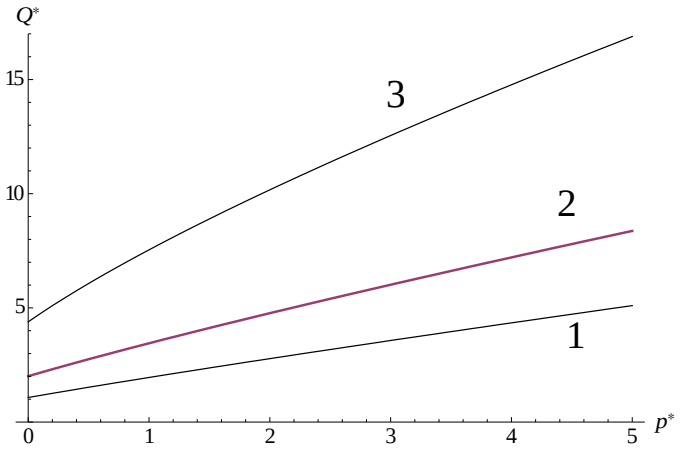


Fig.5. Leaky pipe discharge as a function of pressure in the pipe.

The computed value of $Q^*$ is used to calculate $H^*$ and then $h^*$. For example, let us consider a sandy soil with $h_c$=1.5 m and $k$= 0.3 m/day, irrigated by a mole hole of a radius $R$=4.5 cm and pressure of 30 kPa ($p_p$=3 m, $p_p^*$=1.5). Then, from curve 2 in Fig.5, $Q^*$ =4.77 ($Q$=2.15 m$^2$/day per meter in the direction perpendicular to the plane of Fig.1a), $H^*$=1.05 ($H$=1.58 m) and the dimensionless total head along the hole contour $h^*=p^* +H^*+1=3.55$.

## *2.4 Isobars*

Similarly to Raats (1971), we plot the isobaric contours, which, as Raats correctly noticed, can not be used for modeling the pressurized leaky pipes or mole hole contours (contrary to Philip's original statement). Indeed, any line of contact between a free water body (e.g. water in a pipe or furrow) and soil is a line of constant total head, not pressure head (see e.g. Warrick and Zhang, 1987, Siyal and Skaggs, 2009). The isobars are, however, necessary for three main purposes: a) abstraction of soil moisture by plant roots is controlled by the pressure head; b) determination of the zero-pressure isobar is important for detection of validity of the P-69 model and its stitching with R-38; c) in transient SI seepage, the zero-pressure contour is an important design characteristic (see e.g. Thorburn et al., 2003, their Fig.1). Irrigation engineers focus

mainly on tracking the wetting front (capillary fringe in the GA model) and do not even mention that the “saturated bulb”, demarcated by this contour, also expands with time and asymptotically attains the R-38 zero-isobar shape.

From eqn.(A4) we express $\tau$ through the Zhukovsky function:

$$\tau = \left( \frac{1+\exp\frac{2\pi F_z}{Q}}{1-\exp\frac{2\pi F_z}{Q}} \right)^2 = \left( \coth\frac{\pi F_z}{Q} \right)^2 \tag{4}$$

Obviously, $z = \frac{w}{ik} - \frac{F_Z}{ik}$.

Then using eqns. (A3) and (4) we get

$$z = \frac{iF_z}{k} - \frac{iQ}{2\pi k}\log\left[ \left( \frac{1+\exp\frac{2\pi F_z}{Q}}{1-\exp\frac{2\pi F_z}{Q}} \right)^2 - 1 \right] = \frac{iF_z}{k} + \frac{iQ}{\pi k}\log\sinh\frac{\pi F_z}{Q} \tag{5}$$

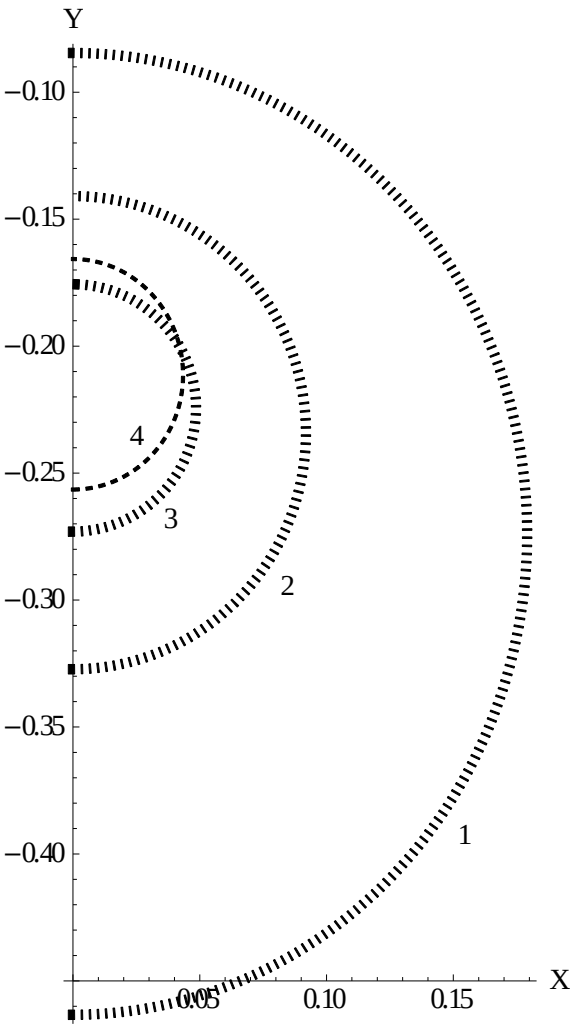


Fig.6. Three isobars (dotted lines) and one equipotential contour (dashed line).

For isobars $u=\mathrm{Re}[F_z]=-k(p+h_c)=c_1=$ const$<0$, i.e. their images in Fig.2b are vertical segments shown by dotted lines, in particular, the "water table" $u=-kh_c$ $(p=0)$. Therefore, in eqn.(5) we set $F_z=c_1+iv$ where $v$ is a parameter in the range $0 \le v \le Q/2$. Then, similarly to what we have done with the flow net, for a fixed $c_1$ we separate the real and imaginary parts by the **Re** and **Im** routines of *Mathematica* and plot the isobars by the **ParametricPlot** routine. Fig.6 shows the isobars for $h_{cd}$ = 0.2, and $C_1=c_1/Q$ = -0.3, -0.2 and -0.1 (dotted curves 1-3). Curve 2 is, obviously, the "water table". For comparisons, curve 4 (dashed line) in Fig.6 is a contour of constant total head $h_d$ = 0.1. It intersects curve 3 and hence only the part of curve 3 outside the domain encompassed by curve 3 (interior of the leaky pipe) should be retained as a

physically meaningful isobar of pore pressure in the soil, of course, if the pipe is at the selected total pressure head of $h_d$ = 0.1.

### *2.5 Isochrones*

Philip (1984) pioneered in calculation of the travel time of water particles emitted from a point source and moving along streamlines. He used a Lagrangian approach and evaluated the position of marked particles released at time moment $t$=0 and stroboscopically mapped at snapshots $t=T_s$. The loci of these front particles (isochrones) are key parameters in SI design and irrigation scheduling (see e.g., Sepaskhah and Chitsaz, 2004, Zur, 1996).

If all streamlines are marked by these particles, they make an isochronic contour, also called a green-amptian imbibition front. The dimensional travel time in saturated (Kacimov and Tartakovsky, 1994, Kacimov and Yakimov, 2010) or tension-saturated flows is expressed by the formula:

$$T_s(\phi_m,\phi_M,\psi)=m\int_{\phi_m}^{\phi_M}\frac{d\mu}{|V(\mu,\psi)|^2}, \qquad (6)$$

where $m$ is porosity, $\varphi_m$ and $\varphi_M$ are the minimum and maximum potentials from which a particle moves along a selected streamline.

We determined isochrones in the following manner: we fixed $\phi_m$ (lower limit of integration) which corresponds to a leaky pipe contour. Then we fixed $\psi$, $0<\psi<1/2$. Next, we fixed $T_s$ and solved the nonlinear eqn.(6) with respect to $\phi_M$ by the help of the **FindRoot** and **NIntegrate** *Mathematica* routines (we recall that the velocity field is determined by eqn.(A7)). The found value of $\phi_M$ we put back into the parametric equations of streamlines, eqn.(A5), and calculated the locus of the particle. Then we repeated the process for all streamlines at a given $T_s$.

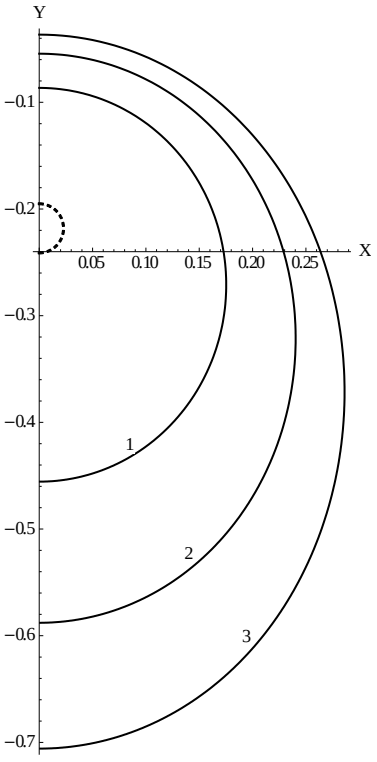


Fig.7. Three isochrones of marked particles emitted from R-38 source and travelling along streamlines.

Fig.7 shows the isochrones in dimensionless coordinates (*X*,*Y*) for $\phi_m = -0.2$, $T_{sd} = 0.1, 0.2$ and 0.3 (curves 1-3, correspondingly) where $T_{sd}=T\ k\ /(mQ)$ is dimensionless time. In fertigation i.e. when solutes are suddenly injected into a leaky pipe which already seeps in a steady-state regime, advection into the soil and demarcation of isochrones are important for modeling of the piston-type propagation zone.

## *2.6 Geometrical Non-circularity of Equipotentials*

As is apparent from Figs.3 and 6, the near-source equipotentials, which can be considered as tube contours, are not ideally semicircular (for example, contour 4 in Fig.3 is bomb-shaped and contour 3 is pear-shaped). Even if they are close to semicircles, their "centres" Ce may not coincide with point *A* (see Fig.1b which zooms the near-source equipotentials) but are rather upwelled. These "eccentricity" and "*y*-elongation" have been quantified by Fujii and Kacimov (1998) and Obnosov et al. (2010). Here we define the vertical and horizontal "diameters" of

equipotentials as $d_v=Y_{Eu}-Y_{Ed}$ and $d_h=2X_P$ where $P$ is the point of maximal abscissa of the tube contour (see Fig.1a,b) according to eqn. (A5). We use **FindMaximum** of *Mathematica* to calculate $X_P$. The eccentricity and ovality are defined as $e=(Y_{Eu}+Y_{Ed})/2+log2/\pi$ (see Fig.1b) and $ov=d_h/d_v$ respectively. They are plotted as Fig.8a and Fig.8b respectively.

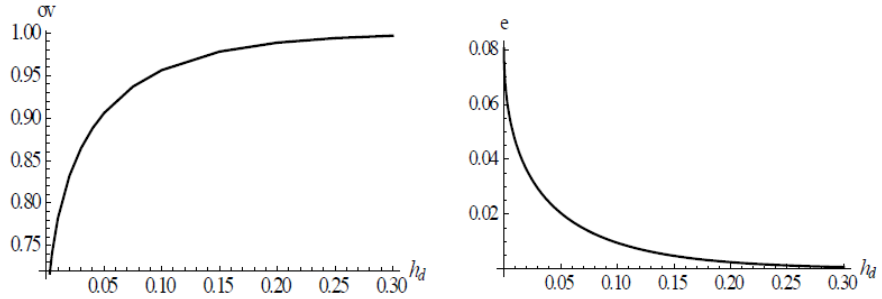


Fig.8. Dimensionless eccentricity ("upwelling") of the hole centre *Ce* as compared with the source depth $Y_A$ in R-38 (left panel). Ratio of the horizontal "diameter" of R-38 ovalic equipotentials to their vertical diameters. (right panel).

As is evident from these figures, at $h_d > 0.2$ the equipotentials generated by a mathematical source are indeed almost circular and point Ce in Fig.1b almost coincides with point A. Figs. 8 are important to know whether the very "linear source" mathematical concept is suitable for mimicking real "leaky" pipes (which are always circular) and if yes, what is the depth of the source to place it in the model to correctly relate to the depth of the physical pipe axis.

## *2.7 Finite Thickness Low-permeable Pipe Walls*

Real leaky pipes are made of clay and the walls, which are about 1 cm thick create an additional hydraulic resistance to seepage (see Gupta et al, 2009 and Siyal and Skaggs, 2009). Obviously, if the wall is too thick or its permeability is too low, then no significant transmission of water from the pipe to the soil roots takes place, i.e. the main purpose of the emitter is defeated and R-38 theory is not applicable.

Now we consider a wall of a finite thickness $\delta$ and hydraulic conductivity $k_w<k$ (Fig.1c). Fig.1c zooms the "near field" ("formation damage" in the vernacular of reservoir engineering applications) zone of the porous annulus of the wall. We neglect the eccentricity (*Ce* coincides with *A* in Fig.1c) and ovality (*ov*=1). We assume that the dimensional total hydraulic head in the wall $h_w(r)$ ($R<r<R+\delta$, where $r$ is the radial coordinate in Fig.1c) decreases from zero at the internal wall circumference $E_{u0}P_0E_{d0}E_{u0}$ to a constant negative value $h_e$ at the external wall circumference $E_uPE_dE_u$ which is in perfect contact with the ambient soil. Then upon applying the Darcy law (namely, the well-known Thiem solution in well hydraulics, see e.g. Houben, 2015) for seepage through the wall we get:

$$h_e = -\frac{Q}{2k_w\pi}\log\left(1+\frac{\delta}{R}\right) \tag{7}$$

The pressure head $p_w(r)$ in the wall annulus is defined as

$$p_w = p_p + h_w - y \tag{8}$$

We apply eqns.(7) and (8) to point $E_u$ in Fig.1c and get at this point

$$p_w = p_p - R - \delta - \frac{Q}{2k_w\pi}\log\left(1+\frac{\delta}{R}\right) \tag{9}$$

Clearly, there should be $p_w > -h_c$ in eqn.(9) in order to apply the R-38 theory of tension-saturated seepage in the soil, i.e. too clayey or too thick walls are not allowed. If the inequality holds the whole above presented analysis for a "bare-foot mole hole" is replicated in the "far-field" zone, with an adjusted value of the total head along the wall-soil contact circle.

## 3. **Quasilinear model of unsaturated flow**

In this section we compare P-69 for a buried line source emitting water in a homogeneous infinite soil massif ($a=\infty$ in Fig.1a). The P-69 model assumes a genuinely unsaturated flow with an unsaturated hydraulic conductivity, $k_{un}$, as an exponential function of the pressure head (negative everywhere in the flow domain), $p$ :

$$k_{un} = k \exp[\alpha\ p] \qquad (10)$$

where $\alpha$ =*const*>0 is the so-called sorptive number, which is usually related to the air-entrance capillary pressure head, $p_a$ , as $\alpha = 1/\ p_a$ and to the wetting capillary pressure head, $p_w$, at the interface of an imbibition front as $\alpha = 1/(2\ p_w)$ (see Ahuja et al., 1989 and Whisler and Bouwer, 1970 for details and tabulated values for different types of soils). The positive constants $p_a$ and $p_w$ are the parameters of the Green-Ampt 1-D transient drainage or infiltration models, respectively.

In P-69 the Kirchhoff potential, $\theta$, is introduced as:

$$\theta = \int_{-\infty}^{p} k_{un}(p) d\ p = \frac{k_{un}[p(x,y)]]}{\alpha} \qquad (11)$$

Using eqn.(10) in eqn.(11), the master (Richards') equation is reduced to the following linear PDE (specifically, ADE) and Darcian velocity:

$$\Delta\theta = \alpha \frac{\partial\theta}{\partial z_p}, \qquad V_x = -\frac{\partial\theta}{\partial z_p}, \quad V_z = \alpha\theta - \frac{\partial\theta}{\partial z_p} \qquad (12)$$

where $\Delta$ is the Laplacian operator and the P-69 coordinate system $x_p A z_p$ originates at the source in Fig.1a, the $z_p$ -axis oriented vertically down, $V_x$ and $V_z$ are the horizontal and vertical velocity components. Obviously, as compared with R-38, $x_p = x$, $z_p = -y+H$ (see the previous section). Then in dimensional variables, for a source of intensity $Q$ placed at point A in Fig.1a, solution in P-69 is:

$$\theta = \frac{Q}{2\pi} \exp[\alpha z_p / 2] K_0 \left[ \sqrt{(\alpha x_p / 2)^2 + (\alpha z_p / 2)^2} \right] \qquad (13)$$

where $K_0$ is the Macdonald function of zero order.

Since P-69, plethora of work has been published on subsurface sources (see e.g. Raats, 1977, Warrick and Lomen, 1977) modeled by eqn.(12). The problem with the source solution, eqn.(13), is in the near-source zone. Physically, for a leaky pipe with a skin-effect or mole-type

emitter without a wall, the gauge pressure head in the vicinity of the source is positive, i.e. a zone of full saturation of positive $p$ shells the mathematical singularity. In this zone, the governing equation (12) and solution (13) are not valid. Lockington et al., 1989, Martinez and McTigue, 1991, Philip, 1992, Pullan and Hannaford, 1991, Warrick, 1993, Warrick and Zhang, 1987 worked through this model drawback and demarcated a "near-field" positive-$p$ zone, where the Laplace equation for pressure (alternatively, velocity potential or stream function) has to be solved, and a "far-field" negative-$p$ zone where eqn. (12) holds. Conjugation of flows in these two zones has been accomplished only numerically or in an approximate manner, for example, by specifying the shape of this zone (e.g. an ellipse in 2-D or spheroid in 3-D SI flows).

Philip (1990) advocated the quasilinear model which seems mathematically easier than the free boundary problem of R-38. Philip (1992) pointed out, however, that even in his quasilinear model the interface between a saturated near-source and unsaturated far-field (in our case of Fig.1a the line $I_1I_2$) is an unknown free boundary. Moreover, in transient problems of infiltrometry, Phlip (1993) had to recur to the Green-Ampt model with an evolving bulb-shaped capillary fringe (free surface) encompassing a disk source.

It is noteworthy that for a sink, either line or point, as well as an impermeable barrier of a moderate size there is no such impediment to apply eqn.(12) and its simplest Green function (13) (of course, with a negative $Q$) in the vicinity of the singularity and, consequently, to model suction of moisture to, say, a vacuum-drain (see e.g., Fujii and Kacimov, 1998, Kacimov, 2007, Raats, 1977). We also emphasize the advantage of the R-38 model as compared with the Philip model: the same Laplace equation holds in both saturated and tension-saturated zones of Fig.1a and only the external free surface (capillary fringe boundary) is determined.

Now, we follow the Warrick and Zhang (1987) path in stitching R-38 with P-69. We note that solution for a steady-state GA flow from a semi-circular furrow with a capillary

fringe used in Warrick and Zhang (1987) is generally speaking incorrect as proved by Kacimov (2003).

In Fig.1a we sketched the contour $I_1I_2$ as a "water table" at which the pressure head $p$=0 and in Fig.6 this isobar (curve 2) is computed. We use the R-38 solution in the positive-$p$ zone of Fig.1a and try to use P-69 in the exterior. For this purpose we have to compare the isobars $p$=0 of the two models (P-69 and R-38) for the same soil and emitter, i.e. the same $Q$, $k$ and capillary constants. From eqns. (10)-(11), in the P-69 model the pressure head is:

$$p=\frac{1}{\alpha}\log\frac{k_{un}}{k}=\frac{1}{\alpha}\log\frac{\alpha\theta}{k} \tag{14}$$

From eqn.(14) along the zero-pressure isobar $\theta = k/\alpha$ and therefore from eqn. (13) we get

$$1=\frac{\alpha Q}{2\pi k}\exp[\alpha z_p/2]K_0\left[\sqrt{\left(\alpha x_p/2\right)^2+\left(\alpha z_p/2\right)^2}\right] \tag{15}$$

in dimensional variables. To convert (15) to dimensionless quantities of Fig.6 we have to relate two physical constants, $\alpha$ and $h_c$, of the two models. We write $\alpha=1/(c_a\ h_c)$ where $c_a$ is a conversion number to be found. We introduce dimensionless variables $Z=-k\ z_p/Q$, $X=k\ x_p/Q$, $h_{cd}=k\ h_c/Q$. In these variables eqn.(15) is reduced to a dimensionless form:

$$c_a h_{cd}=\frac{1}{2\pi}\exp[Z/(2c_a h_{cd})]K_0\left[\sqrt{\left(X/(2c_a h_{cd})\right)^2+\left(Z/(2c_a h_{cd})\right)^2}\right] \tag{16}$$

We used the **ContourPlot** routine of *Mathematica* to plot the isobars according to eqn. (16) for $h_{cd}$=0.2 and $c_a$=1, 2, 1.5 and 2.5, solid-line curves 1-4 in Fig.9, correspondingly. The dotted line there is the R-38 isobar $p$=0 (curve 2 from Fig.6, re-plotted in the coordinates of this section).

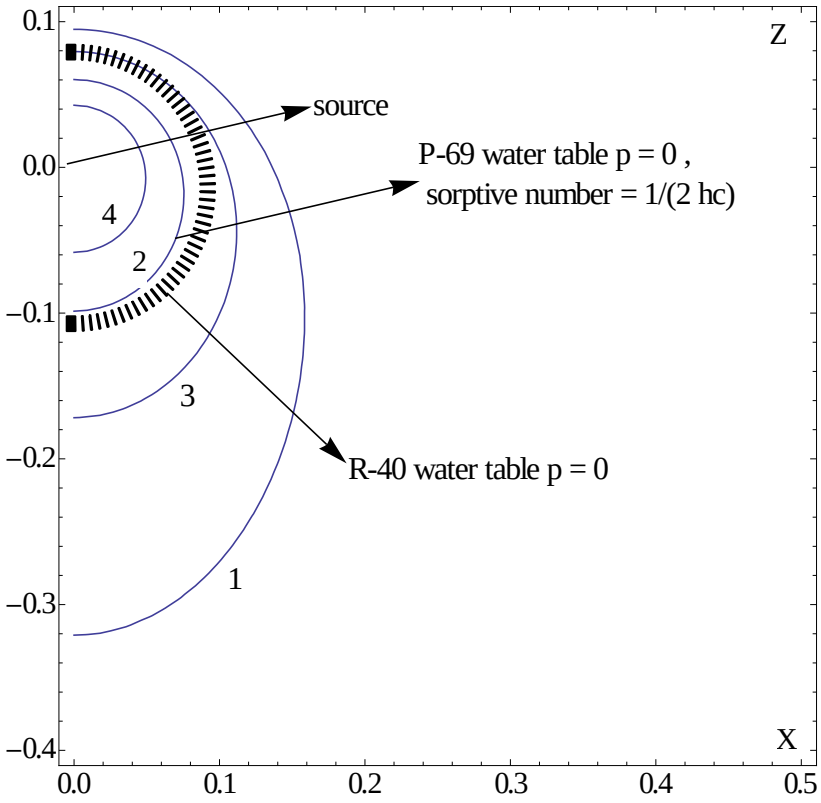


Fig.9. Comparison of the "water table" in R-38 and P-69 for adjusted values of capillary constants.

As is clear from Fig.9, $c_a$=2 gives the best fit between R-38 and P-69 ovalic "water tables". This relation $\alpha=1/(2h_c)$ is in congruity with how Whisler and Bouwer (1970) linked the Green-Ampt and Philip models. We repeat that the original Vedernikov's (1939) parameter $h_c$, widely used in R-38, PK-62,77 for other free boundary, tension-saturated flows, is measured as a static height of capillary rise in a column, while $\alpha$ is measured in drainage or imbibition experiments, e.g. by tension infiltrometers.

### *3.1 Two Quasilinear Isochrones*

Philip's (1984) gave stellar mathematical derivations of travel time for marked particles emitted from a quasilinear point source. However, he assumed a constant moisture content along streamlines, surmising that this assumption does not affect much isochrones. In this subsection we find the travel time of tracer particles for a line source, eqn.(13), for two vertical streamlines

only (AB and AC in Fig.1a) but taking into account a progressive decrease of the moisture content from the source to an absolutely dry "infinity".

The travel time, *T(s),* along a fixed streamline of a steady quasilinear flow is:

$$T = \int_0^s \frac{m(s)}{V(s)} ds \qquad (17)$$

where *m(s)* is now a varying volumetric moisture content, *s* is the streamline arc coordinate, *V* is the magnitude of the quasilinear Darcian velocity and tracking starts from the point of release of the particle. This starting point should be, as we discussed above, within the realm of the quasilinear theory, e.g. originate at the isobar *p=0*, curve 2 in Fig.9. However, this zone of invalidity of the P-69 theory is usually ignored due to high *V* near the source, i.e. the journey of particles is assumed to start from the source itself (Philip, 1984). In eqn. (17), *m(s)* decreases from a wetter to drier zone (numerator in the intergand) but $k_{un}$ decreases in this direction (denominator in the intergand).

We introduce Philip's dimensionless coordinates $V_{zd}=V_z/k$, $z_d=\alpha z/2$, $\theta_d=\alpha\theta/k$, $Q_d=Q\alpha/k$, $T_d=Tk/(2\alpha)$. The vertical velocity component becomes:

$$V_{zd} = \theta_d - \frac{1}{2}\frac{\partial \theta_d}{\partial z_{pd}} \qquad (18)$$

Philip differentiated a correspondingly dimensionalized eqn.(13) and obtained from eqn.(18):

$$V_{zd} = \frac{Q_d \exp[z_d]}{4\pi}\left( K_0[0,|z_d|] + \frac{z_d}{|z_d|} K_1[0,|z_d|] \right) \qquad (19)$$

where $K_1$ is the Macdonald functions of first order (both $K_0$ and $K_1$ are routines of *Mathematica*).

Averyanov's formula (see e.g. PK-77, Al-Maktoumi et al., 2015) for unsaturated hydraulic conductivity is: $k_{un}=k\ m^{3.5}$ (a residual moisture content is assumed to be zero) and hence

$m=\theta_d^{1/3.5}$. We put this expression, as well as eqn.(19), into the numerator and denominator of eqn. (17) (respectively) and use the **NIntegrate** routine of *Matheamtica* to evaluate the travel time along the rays AB (negative $z_{pd}$ ) and AC (positive $z_{pd}$).

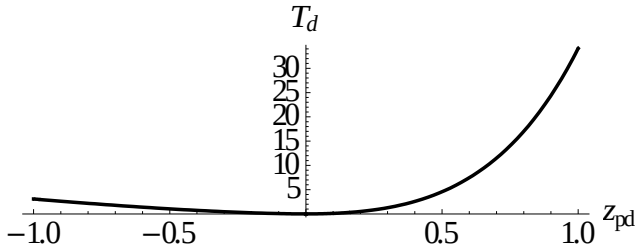


Fig.10. Dimensionless time of travel of marked particles along two vertical streamlines in P-69, with nonconstant moisture content along these rays.

The results are shown in Fig. for $Q_d$=1 (for other given source strengths, scaling is through a constant coefficient $Q_d^{1/3.5-1}$). Trivially, from Fig.10 we see a huge difference in travel time along the ascending and descending vertical streamlines. What is less obvious: when we, as Philip (1984) did, took $m=m_{av}=const$, $0<m_{av}<1$ along both streamlines and integrated eqn.(13), the results were quite different from Fig.10.

## 4. Conclusions and Perspectives

Modeling seepage from buried line sources is important for proper design of SI widely used in crop production, especially, in arid or semi-arid regions like Oman, Kansas or California. The recent trend to rely on HYDRUS2-,3-D and other purely numerical packages should be corrected by involving analytical solutions, stemming from R-38 and P-69.

Using a modern computer algebra software, we extended the R-38 solution: found the flow net, isobars in the positive-pressure and tension-saturated zones, distribution of the Darican velocity and resultant force acting on soil particles, travel time along streamlines, the seepage discharge for barefoot water-emitting hole and leaky pipe. We followed the Warrick and Zhang (1987) approach to conjugate Laplace's equation and ADE and found which sorptive number in

the Philip model gives the best fit with the capillary number in the Vedernikov-Greeen-Ampt model for 2-D tension-saturated flows.

R-38 and P-69 soil is unbounded in all directions. In practical SI, there is often a confining low-permeable layer and water-sucking (evapotranspiring) soil surface such that optimization problems have to be solved by agricultural engineers: where, in between the two horizons, to place a source of SI to maximize the advantages and minimize the drawbacks of this irrigation technology? The possibly too small an extent of the wetted zone from on emitting source, would require that an array of emitters to be used (as e.g. in Elnesr et al., 2015). Analytical solutions, intertwined with HYDRUS modeling, will be instrumental in answering this question. In this case Strack's (1989) solutions (with water table converted to capillary fringe free boundaries) should be used.

**ACKNOWLEDGMENTS**

This work was supported by TRC grant ORG/EBR/15/002 (Oman), Russian Foundation for Basic Research grant No 13-01-00322 and through a special program of the Russian Government supporting research at Kazan Federal University. Helpful comments by two referees are appreciated.

We declare that we comply with the AGU Data Policy. Readers can find the data that support or underlie the conclusions presented in the manuscript in the cited references. No unavailable data are used in the manuscript. No data in the manuscript are in any repository. The model data (computer algebra outputs, including the code) are available from the authors upon request. If the editor-in-chief recommends, we can make the code available by posting code on publicly accessible sites such as GITHUB or other code repositories.

## APPENDIX

R-38 obtained solution for a general case of evaporation from the fringe surface with a "background" flow from beneath (from a subjacent aquifer). To bridge with P-69, we ignore evaporation and ascending flow from the aquifer.

We introduce Cartesian coordinates *xBy* where *B* is the apex of the capillary fringe. The complex physical coordinate is $z=x+i\,y$. Due to symmetry we consider the right half of the flow domain, $G_z$. We introduce a complex potential

$$w = \varphi + i\psi\,, \qquad (A0)$$

where $\varphi = -kh(x,y)$ is a potential ofthe Darcian velocity $\vec{V} = -k\nabla h = \nabla\varphi$, $h$ is the total hydraulic head and $\psi$ is the stream function. We stress that in (A0) the potential is opposite in sign of the piezometric head. We recall that according to the Vedernikov-Green-Ampt model $k$ is constant within $G_z$ and is nil outside $G_z$.

The apex *B* is a fiducial point where $w=iQ/2$ i.e. we assume $h_B=0$. Then the pressure head in the soil is defined as

$$p = -h_c - (\varphi/k + y) \qquad (A1)$$

The functions $h, \varphi, p, \psi$ and all their linear combinations are harmonic in $G_z$ i.e. satisfy the Laplace equation.

We (as R-38 did) start with the case of no skin-effect (no wall resistance to seepage into the soil). This is mathematically and physically identical to the so-called bare-foot wells and laterals in the petroleum industry (no casing of horizontal wells drilled through a hard rock).

Then, from reading of an imaginary piezometer in Fig.1a and eqn. (A1) we have

$$h_p = p_p + h_c - H \qquad (A2)$$

where the source depth *H* (counted from point *B*) is a part of solution, with $H<a$.

The complex potential domain, $G_w$, is a strip of width $Q/2$ (Fig.2a). We introduce the Zhukovsky function $F_Z=w-ikz$, $\mathrm{Re}[F_Z]=u=\varphi+ky$, $\mathrm{Im}[F_Z]=v=\psi-kx$. The corresponding domain $G_F$ is a half-strip depicted in Fig.2b.

We map conformally $G_w$ onto the upper half-plane of an auxiliary plane $\tau=\xi+\imath\eta$ (Fig.2c) with the correspondence of points $B\to 0$, $A\to 1$, $C\to\infty$. We use the logarithmic function:

$$w = \frac{Q}{2\pi}\log(\tau - 1) \qquad \text{(A3)}$$

where the branch of logarithm is fixed by the condition $0 < \arg(\varsigma - 1) < \pi$.

We also map conformally $G_F$ onto the same half-plane by the Schwartz-Christoffel formula as:

$$F_Z = \frac{Q}{2\pi}\int_0^{\tau} \frac{d\tau}{(\tau - 1)\sqrt{\tau}} + \frac{iQ}{2} = \frac{Q}{2\pi}\log\frac{\sqrt{\tau} - 1}{\sqrt{\tau} + 1} \qquad \text{(A4)}$$

where the branch of the last analytic function is fixed in the upper half-plane by the condition of its negativity at $\tau = \xi > 1$.

Combining eqns. (A3) and (A4) gives

$$z(\tau) = \frac{w(\tau) - F_z(\tau)}{ik} = \frac{-iQ}{k\pi}\log(\sqrt{\tau} + 1) \qquad \text{(A5)}$$

From eqn.(A5) at $\tau$=1 (source at $z$=-$iH$)

$$H = \frac{Q}{\pi k}\log 2 \qquad \text{(A6)}$$

We introduce a holomorphic function $V$=$V_x$ - $iV_y$ , complex conjugated with the Darcian velocity, which has the horizontal and vertical components $V_x$ and $V_y$. Then from eqns. (A3) and (A5)

$$V(\tau) = \frac{dw}{dz} = \frac{dw}{d\tau} / \frac{dz}{d\tau} = \frac{ik\sqrt{\tau}}{\sqrt{\tau} - 1}, \qquad \text{(A7)}$$

From eqn.(A3)

$$\tau = 1 + \exp\frac{2\pi w}{Q} \qquad \text{(A8)}$$

and we get $z$, $V$ and $F_z$ as functions of $\varphi, \psi$.

We note that $G_F$ in Fig.1c is a limiting case of the tetragone shown by PK-77 in her Fig.89в which is a characteristic domain for flow generated by a source superimposed with an ascending

background flow from a deep formation where an infinitely-high pressure is maintained (see R-38 for details). The R-38 tetragon transforms into our half-strip in Fig.2b as the evaporation rate approaches zero and pressure head at infinity decreases from positive infinity to $p=-h_c$. It is noteworthy that R-38 results were – via PK-62,77 – utilized not only in SI but also in geotechncial engineering (see e.g. Mei, 1977).

## References


Al-Maktoumi, A., Kacimov, A., Al-Ismaily, S. and Al-Busaidi, H., 2015. Infiltration into two-layered soil: The Green-Ampt and Averyanov models revisited. Transport in Porous Media, 109, 169-193,

Al-Rawahy, S., Rahman, H.A., and Al-Kalbani, M.S., 2004. Cabbage (*Brassica oleracea L.*) response to soil moisture regime under surface and subsurface point and line applications. Inerntnl. J. Agriculture & Biology, 6, 1093–1096.

Ashrafi, S., Gupta, A.D., Babel, M.S., Izumi, N. and Loof, R., 2002. Simulation of infiltration from porous clay pipe in subsurface irrigation. Hydrol. Sci. J., 47 (2), 253-268.

Ayars, J.E., Fulton, A. and Taylor, B., 2015. Subsurface drip irrigation in California—Here to stay? Agricultural Water Management, 157, 39–47.

Camp, C.R., 1998. Subsurface drip irrigation: a review. Trans. ASAE, 41 (5), 1353–1367.

Chu, S.T., 1994. Green-Ampt analysis of wetting patterns for surface emitters. J. Irrigation and Drainage Engrg. ASCE, 1994, 120(2): 414-421

Cook, F.J., Thorburn, P.J., Bristow, K.L. and Cote, C.M., 2003. Infiltration from surface and buried point sources: the average wetting water content. Water Resources Research, 39(12), 1364.

Diamantopoulos, E. and Elmaloglou, S., 2012. The effect of drip line placement on soil water dynamics in the case of surface and subsurface drip irrigation. Irrigation and Drainage, 61, 622–630.

El-Nesr, M.N., Alazba, A.A., and Simunek, J., 2014. HYDRUS simulations of the effects of dual-drip subsurface irrigation and a physical barrier on water movement and solute transport in soils. Irrigation Science, 32, 111–125.

Elnesr, M.N., Alazba, A.A., Zein El-Abedein, A.I., and El-Adl, M.M. ,2015. Evaluating the effect of three water management techniques on tomato crop. PLoS ONE, 10(6): e0129796. doi:10.1371/journal. pone.0129796

Emikh, V.N., 1999a. Seepage flow from subsurface sources. Fluid Dynamics, 34 (2), 218-228.

Emikh, V.N., 1999b. Intercepting drainage in flow from a subsurface source. Fluid Dynamics, 34(3), 363-369.

Fujii, N. and Kacimov, A.R., 1998. Analytically computed rates of seepage flow into drains and cavities. International J. for Numerical and Analytical Methods in Geomechanics, 22, 277-301.

Gupta, A.D., Babel, M.S. and Ashrafi, A., 2009. Effect of soil texture on the emission characteristics of porous clay pipe for subsurface irrigation. Irrigation Science, 27, 201–208.

Hawes, M.C., Bengough, G., Cassab, G., and Ponce, G., 2003. Root caps and rhizosphere. J. of Plant Growth Regulation, 21, 352–367.

Houben, G.J. 2015. Review: Hydraulics of water wells—head losses of individual components. Hydrogeol J. 23(8), 1659-1675. DOI 10.1007/s10040-015-1313-7

Kasimov, A.R., 1992. Minimum dimension of total saturation bubble around an isolated source. Fluid Dynamics, 27, 886-889.

Kacimov, A.R., 2003. Discussion on a technical note by Swamee P.K. and Kashyap D. "Design of minimum seepage-loss nonpolygonal canal sections". J. Irrigation and Drainage Engrg. ASCE, 129(1), 68-69.

Kacimov, A.R., 2004. Capillary fringe and unsaturated flow in a reservoir porous bank. J. Irrigation and Drainage Engrg. ASCE, 130, 403-409.

Kacimov, A.R., 2007. Dipole-generated unsaturated flow in Gardner soils. Vadose Zone J., 6, 168-174.

Kacimov, A.R. and Tartakovsky, D.M., 1993. Estimation of tracer migration time in ground water flow. Computational Mathematics and Mathematical Physics, 33(11), 1535-1541.

Kacimov, A.R. and Yakimov, N.D., 2009. Minimal advective travel time along arbitrary streamlines of porous media flows: the Fermat-Leibnitz-Bernoulli problem revisited. J.Hydrology, 375, 356-362.

Lamm, F.R. and Camp, C.R., 2007. Subsurface drip irrigation. In "Microirrigation for Crop Production. Design, Operation and Management." Edited by F.R. Lamm, J.E. Ayars and F.S. Nakayama, Elsevier, Amsterdam, 473-551.

Lamm, F.R., Bordovsky, J.P., Schwankl, L.J., Grabow, G.L., Enciso-Medina, J., Peters, R.T., Colaizzi, P.D., Trooien, T.P., and Porter, D.O., 2012. Subsurface drip irrigation: Status of the technology in 2010. Transactions of the ASABE, 55 (2), 483-491.

Lockington, D., Hara, M., Hogarth, W. and Parlange, J.-Y., 1989. Flow through porous media from
a pressurized spherical cavity. Water Resources Research, 25, 303-309.

Lubana, P.P.S. and Narda, N.K., 2001. Modelling soil water dynamics under trickle emitters: A review. J. Agricultural Engineering Research, 78, 217–232.

Martínez, J. and Reca, J., 2014. Water use efficiency of surface drip irrigation versus an alternative subsurface drip irrigation method. J. Irrigation and Drainage Engineering ASCE. DOI: 10.1061/(ASCE)IR.1943-4774.0000745

Martinez, M.J., and McTigue, D.F., 1991. The steady distribution of moisture beneath a two-dimensional surface source, Water Resources Research, 27, 1193–1206.

Mei, C.C., 1977. Leakage of groundwater through a slot in sheet pile. J. of Hydraulic Research, 15(3), 253-259, DOI: 10.1080/00221687709499646

Mmowala, K. and Or, D., 2000. Root zone solute dynamics under drip irrigation: A review. Plant and Soil, 222, 163–190.

Naglič, B., Kechavarzi, C., Coulon, F., and Pintar, M. , 2014. Numerical investigation of the influence of texture, surface drip emitter discharge rate and initial soil moisture condition on wetting pattern size. Irrigation Science, 32, 421–436.

Nikolskii, I.S., 1961. Seepage of air from a horizontal drain laid under a reservoir bottom. Fluids Dynamics, 181–183 (in Russian).

Obnosov, Yu.V., Kasimova, R.G., Al-Maktoumi, A., and Kacimov, A.R., 2010. Can heterogeneity of the near-wellbore rock cause extrema of the Darcian fluid inflow rate from the formation (the Polubarinova-Kochina problem revisited)? Computers & Geosciences, 36, 1252–1260.

Polubarinova-Kochina, P.Ya., 1962. Theory of Ground Water Movement. Princeton University Press, Princeton. Second edition of the book in Russian is published in 1977, Nauka, Moscow.

Philip, J.R., 1968. Steady infiltration from buried point sources and spherical cavities. Water Resources Research, 4, 1039–1047.

Philip, J.R., 1969. Theory of infiltration. Adv. Hydroscience, 5, 215–296.

Philip, J.R., 1984. Steady infiltration from circular cylindrical cavities. Soil Sci. Soc. Am. J., 48, 270-278.

Philip, J.R., 1989. Multidimensional steady infiltration to a water table. Water Resources Research, 25, 109-116.

Philip, J.R., 1990. How to avoid free boundary problems, in Free Boundary Problems: Theory and Applications, vol. 1, Res. Notes Math., vol. 185, edited by K.H. Hoffmannn, and J. Sprekels, pp. 193–207, Longman, New York.

Philip, J.R., 1992. What happens near a quasi-linear point source? Water Resources Research, 28, 47-52.

Philip, J.R., 1993. Approximate analysis of falling-head lined borehole permeameter. Water Resources Research, 29, 3763–3768.

Pullan, A.J., and Hannaford, R.H., 1991. Pressurized steady state flows from horizontal cylindrical cavities. Water Resources Research, 27, 797–80.

Raats, P.A.C., 1968. Forces acting upon the solid phase of a porous medium. Z. Angew. Math. Phys., 19, 606-613.

Raats, P.A.C., 1970. Steady infiltration from line sources and furrows, Soil Sci. Soc. Amer. Proc.,
34, 709–714.

Raats, P.A.C., 1971. Steady infiltration from point sources, cavities, and basins. Soil Sci. Soc. Am. Proc., 35, 689–694.

Raats, P.A.C., 1972. Steady infiltration from sources at arbitrary depth. Soil Sci. Soc. Am. Proc., 36, 399–401.

Raats, P.A.C., 1977. Laterally confined, steady flows of water from sources and to sinks in unsaturated soils. Soil Sci. Soc. Am. J., 41, 294–304.

Riesenkampf, B.K., 1938. Hydraulics of groundwater. Part 2. Transactions of Saratov State University, 14(2),181–205 (in Russian).

Sepaskhah, A.R. and Chitsaz, H., 2004. Validating the Green-Ampt analysis of wetted radius and depth in trickle irrigation. Biosystems Engineering, 89 (2), 231–236.

Siyal, A.A., and Skaggs, T.H., 2009. Measured and simulated soil wetting patterns under porous clay pipe sub-surface irrigation. Agricultural Water Management, 96, 893–904.

Siyal, A.A., Van Genuchten, M.T., and Skaggs, T.H., 2013. Solute transport in a loamy soil under subsurface porous clay pipe irrigation. Agricultural Water Management, 121, 73–80.

Strack, O. D. L., 1989. Groundwater Mechanics. Prentice-Hall, Inc., Englewood Cliffs, New Jersey, 1989. 732 pp.

Subbaiah, R., 2013. A review of models for predicting soil water dynamics during trickle irrigation. Irrigation Science, 31 (3), 225-258.

Teeluck, M. and Sutton, B. G. , 1998. Discharge characteristics of a porous pipe microirrigation lateral. Agricultural Water Management, 38(2), 123−134.

Thorburn, P.J., Cook, F.J., and Bristow, K.L., 2003. Soil-dependent wetting from trickle emitters: implications for system design and management. Irrigation Science, 22(3), 121-127.

Vedernikov, V.V., 1939. Theory of Seepage and Its Applications to Problems of Irrigation and Drainage. Moscow-Leningrad, Gosstroiizdat (in Russian).

Warrick, A.W., 1993. Unsaturated-saturated flow near a quasi-linear line source. Water Resources Research, 29, 3759–3762.

Warrick, A.W. and Lomen, D.O. , 1977. Flow from a line source above a shallow water table. Soil Sci. Soc. Am. J., 41, 849–852.

Warrick, A.W. and Zhang, R., 1987. Steady two-and three-dimensional flow from saturated to unsaturated soil. Advances in Water Resources. 10, 64-68.

Wolfram, S. , 1991. *Mathematica*. A System for Doing Mathematics by Computer. Addison-Wesley, Redwood City.

Zur, B., 1996. Wetted soil volume as a design objective in trickle irrigation. Irrigation Science, 16, 101–105.

**Abbreviations**

1) ADE= advective dispersion equation
2) P-69= reference to

   Philip, J.R., 1969. Theory of infiltration. Adv. Hydroscience, 5, 215–296.

3) PK-62,77= reference to

Polubarinova-Kochina, P.Ya., 1962. Theory of Ground Water Movement. Princeton University Press, Princeton +second edition of the book in Russian (published in 1977)

4) R-38= reference to

Riesenkampf, B.K., 1938. Hydraulics of groundwater. Part 2. Transactions of Saratov State University, 14(2),181–205 (in Russian).

5) SI= subsurface irrigation